Astronomy
&
Astrophysics

SNOC: A Monte-Carlo simulation package for high-z supernova observations

A. Goobar[1], E. Mörtsell[1], R. Amanullah[1], M. Goliath[2], L. Bergström[1], and T. Dahlén[3]

[1] Physics Department, Stockholm University, SCFAB, 106 91 Stockholm, Sweden
[2] Swedish Defence Research Agency (FOI), 172 90 Stockholm, Sweden
[3] Stockholm Observatory, SCFAB, 106 91 Stockholm, Sweden

Abstract. We present a Monte-Carlo package for simulation of high-redshift supernova data, SNOC. Optical and near-infrared photons from supernovae are ray-traced over cosmological distances from the simulated host galaxy to the observer at Earth. The distances to the sources are calculated from user provided cosmological parameters in a Friedmann-Lemaître universe, allowing for arbitrary forms of "dark energy". The code takes into account gravitational interactions (lensing) and extinction by dust, both in the host galaxy and in the line-of-sight. The user can also choose to include exotic effects like a hypothetical attenuation due to photon-axion oscillations. SNOC is primarily useful for estimations of cosmological parameter uncertainties from studies of apparent brightness of type Ia supernovae vs redshift, with special emphasis on potential systematic effects. It can also be used to compute standard cosmological quantities like luminosity distance, lookback time and age of the universe in any Friedmann-Lemaître model with or without quintessence.

Key words. methods: numerical, data analysis, Cosmology: cosmological parameters

1. Introduction

The study of brightness of type Ia supernovae (SNe) at high redshifts has become one of the most important tools in observational cosmology over the last few years (Goobar & Perlmutter 1995; Perlmutter et al. 1999; Riess et al. 1998, 2001), giving the first direct observational evidence for a presently accelerating universe. With the increased capabilities of observing very high-redshift SNe, more comprehensive analysis tools are needed (see, e.g., Mörtsell et al. 2001b).

In this work we describe a Monte-Carlo simulation package called *The SuperNova Observation Calculator* (SNOC) which produces synthetic samples of SN observations that can be used to estimate the accuracy of the magnitude-redshift method for measuring cosmological parameters as well as quantifying the possibility of constraining extragalactic dust properties (Goobar et al. 2002a) or investigating the matter distribution in the Universe (Mörtsell et al. 2001a). For example, SNOC can be used to quantify the deviations in the Hubble diagram of type Ia SNe due to gravitational lensing or dust extinction along the line-of-sight. Tools are also provided to compute the possible contamination of an observational sample by core collapse SNe and the likelihood of observation of multiple (lensed) images from individual high-z SNe (Goobar et al. 2002b).

2. The program

SNOC is a modular `FORTRAN77` program using a random number generator described in Walck (1988). The program produces an ASCII output containing one block of data for each synthetic "event". One event corresponds to one SN. Each SN is characterized by its redshift and SN type (i.e. whether is a type Ia, Ibc, IIn, IIP, IIL or "SN1987A like"). The luminosity distance corresponding to the SN redshift is calculated from the user supplied set of cosmological parameters where we assume a standard Friedmann-Lemaître (FL) universe with arbitrary choice of "dark energy". In order to estimate effects along the line-of-sight, e.g., from gravitational lensing and dust extinction, the light beam is traced backwards in time from the observer to the host galaxy, taking into account the non-homogeneity of the universe and possible intervening matter. This procedure is shown schematically in Fig. 1.

The program sequence is as follows:

- Initialization;
- Read user-supplied parameters (see next section);
- Loop: event generator
  1. Select SN type;
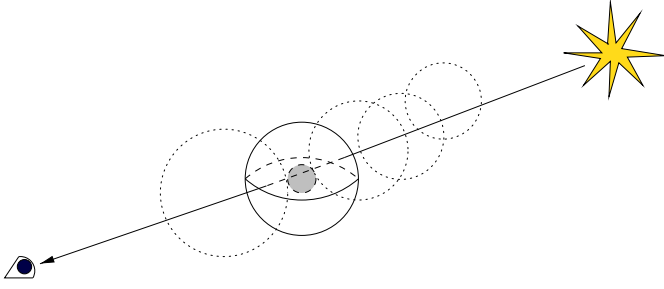
Fig. 1. Schematic view of the ray-tracing technique used in SNOC. The light-beam is traced back-wards in time, from the observer to the host galaxy taking into account the non-homogeneity of the universe and possible intervening matter.

2. Generate SN redshift, z;
3. Calculate distance and lookback time to z;
4. Calculate unperturbed SN lightcurve in a "redshifted" B-band filter[1];
5. Perform ray-tracing
   (a) Calculate gravitational lensing magnification
   (b) Perform differential dust extinction calculation
   (c) Estimate dimming due to exotics, e.g., photon-axion oscillations;
6. Calculate apparent SN brightness in *BVRIJ* filters;
7. Generate host galaxy properties.

3. The user supplied parameters

Table A.1 in Appendix A summarizes the user supplied parameters for the simulation. These include the following main items:

– The number and type of SNe to be generated. The SN types supported are Ia, Ibc, IIn, IIP, IIL and core collapse SNe resembling SN 1987a;
– The redshift distribution to be used. The options include:
  1. Uniform distribution within a chosen range.
  2. Tabulated redshift distribution.
  3. Listed individual redshifts.
  4. Gaussian probability distribution function with given mean value and standard deviation.
  5. Redshift distribution generated from star formation rates [Ref. Dahlén & Fransson (1999)];
– Options for generating the SN lightcurve;
– Cosmological parameters: [$H_0, \Omega_M, \Omega_X, \alpha_X(z)$];
– Gravitational lensing. The user supplies the relative fraction of galaxy halos parametrized as singular isothermal spheres (SIS), Navarro-Frenk-White profiles (NFW), compact objects or spheres with uniform mass density;
– Dust extinction parameters: mean free paths and frequency dependence for host galaxy dust extinction, dust in intervening galaxies and in the intergalactic medium;
– Choice of observed filters (K-corrections);
– Galaxy parameters: luminosity and mass distribution;
– SN search conditions.

---

[1] Transmission function satisfying $B^z(\lambda) = B\left(\frac{\lambda}{1+z}\right)$.

4. The event generator

4.1. Supernova type and redshift distribution

The SN type is selected as either individual type (e.g., "Ia") or a group of SNe (e.g., "core") which generates core collapse SNe with a differential rate as in Dahlén & Fransson (1999) and Dahlén & Goobar (2002).

Several redshift distributions are provided by the code: uniform or Gaussian distributions as well as physically motivated redshift distributions according to:

$$\frac{\mathrm{d}N}{\mathrm{d}z} = \frac{4\pi c d_L^2(z)}{H(z)(1+z)^2} \cdot \frac{r_{SN}(z)}{1+z}, \tag{1}$$

where r_{SN} is the rate of SNe in comoving coordinates. In SNOC we implemented the models of the evolution of the comoving rate of SN explosions in Dahlén & Fransson (1999). In these models an additional user supplied parameter τ indicates the minimum time needed to form the binary systems believed to be the progenitors of type Ia SN explosions. Typical values range from 0.3 to 3.0 billion years.

It is also possible to generate SNe with redshifts from a user provided list of redshifts or user defined distributions.

4.2. The luminosity distance and apparent magnitude: Cosmological models

The luminosity distance and the lookback time to the event are calculated assuming an isotropic and homogeneous universe. In such a FL universe, the scale factor of the universe and thereby the distance estimates are functions of the Hubble constant H_0 and the energy components of the universe (see, e.g., Bergström & Goobar 1999).

The energy density components are treated as perfect fluids characterized by their equation of state, $p_i = \alpha_i \rho_i$. Besides the mass density Ω_M ($\alpha_M = 0$), a second fluid is used in the simulation, Ω_X, with a user specified parameter $\alpha_X(z)$. Thus, SNOC can generate luminosity distances for any choice of Ω_M and Ω_X including the cosmological constant ($\alpha_X = -1$) or a time dependent equation of state parameter as predicted by *quintessence*. In addition to the FL luminosity distance, or *filled beam* distance, the distance in absence of any focusing of the light beam, the *empty beam* distance, is calculated.

The apparent magnitude m of a SN at redshift z, assuming the cosmology $\theta = [\Omega_M, \Omega_X, \alpha_X(z)]$, is given by

$$m(\theta, \mathcal{M}, z) = \mathcal{M} + 5\log_{10}\left[d_L'(\theta, z)\right], \tag{2}$$
$$\mathcal{M} = 25 + M + 5\log_{10}(c/H_0), \tag{3}$$

where M is the absolute magnitude of the SN, and $d_L' \equiv H_0 d_L$ is the H_0-*independent* luminosity distance, where H_0 is the Hubble parameter.[2] Hence, the intercept $\mathcal{M}$ contains the "unwanted" parameters M and H_0 that apply equally to all magnitude measurements [we do not consider evolutionary effects $M = M(z)$]. The H_0-independent luminosity distance d_L' is

---

[2] In the expression for $\mathcal{M}$, the units of c and H_0 are km s^{-1} and km s^{-1} Mpc^{-1}, respectively.

given by

$$d'_L = \begin{cases} (1 + z)\frac{1}{\sqrt{-\Omega_k}} \sin(\sqrt{-\Omega_k}\, I), & \Omega_k < 0 \\ (1 + z)\, I, & \Omega_k = 0 \\ (1 + z)\frac{1}{\sqrt{\Omega_k}} \sin h(\sqrt{\Omega_k}\, I), & \Omega_k > 0 \end{cases} \quad (4)$$

$$\Omega_k = 1 - \Omega_M - \Omega_X, \quad (5)$$

$$I = \int_0^z \frac{dz'}{H'(z')}, \quad (6)$$

$$H'(z) = H(z)/H_0 = \sqrt{(1 + z)^3\, \Omega_M + f(z)\, \Omega_X + (1 + z)^2\, \Omega_k}, \quad (7)$$

$$f(z) = \exp\left[3 \int_0^z dz' \frac{1 + \alpha_X(z')}{1 + z'}\right], \quad (8)$$

where we consider an equation of state with arbitrary z-dependence.

4.3. Ray-tracing

The ray-tracing is discussed in detail in Sect. 5. Here, we summarize its key elements. The light-beam path is divided into "cells" corresponding approximately to average distances between galaxies. Each cell is characterized by

1. The mass density profile, the source of gravitational lensing;
2. The dust density and differential extinction coefficient, treated separately for the actual galaxy in the cell center and the region around it;
3. The average magnetic field and electron density, relevant in exotic scenarios such as the photon-axion oscillation mechanism discussed in Sect. 5.3.

4.4. Supernova and Galaxy apparent magnitudes: K-corrections

The SN and host galaxy apparent magnitudes through a standard (or user specified) broad-band filter is calculated using cross-filter K-corrections as described in Kim et al. (1996). Thus, the apparent magnitude of a SN observed at a redshift z through a filter Y defined through the filter function $S_Y(\lambda)$ becomes:

$$m_Y(z) = \mathcal{M}_X + 5 \log_{10} [d'_L(\theta, z)] + K_{XY}, \quad (9)$$

where the restframe absolute magnitude of the SN is measured in the filter X with a filter transmission function $S_X(\lambda)$.

Assuming a spectral template for each SN type, F_{SN}, and an arbitrary differential attenuation $0 < \epsilon_i(\lambda) < 1$ the K-correction becomes:

$$K_{XY}^i = -2.5 \log_{10}\left(\frac{\int \mathcal{V}(\lambda)S_X(\lambda)\lambda d\lambda}{\int \mathcal{V}(\lambda)S_Y(\lambda)\lambda d\lambda}\right)$$

$$+ 2.5 \log_{10}\left(\frac{\int F_{SN}(\lambda)S_X(\lambda)\lambda d\lambda}{\int F_{SN}(\lambda)\epsilon_i(\lambda)S_Y(\lambda(1 + z))\lambda d\lambda}\right),$$

where the photometry system is normalized in the Vega system, $\mathcal{V}$.

By default, SNOC calculates K-corrections for K_{BY}^i, where Y includes the standard broad-band filters B, V, R, I and J.

In order to assess the color corrections from the various extinction sources we list the results separately:

0) K_{BY}^0: no extinction ($\epsilon_0 = 1$);
1) K_{BY}^1: host galaxy extinction;
2) K_{BY}^2: extinction from galaxies along the line-of-sight;
3) K_{BY}^3: extinction from intergalactic dust;
4) K_{BY}^4: differential effects from photon-axion oscillations.

Finally, K_{BY} (no index) shows the combined effect on the observed magnitudes from all the considered attenuation sources.

Similarly, representative galaxy templates for E, Sbc, Scd and Im galaxies from Coleman et al. (1980) are used to calculate the observed colors of the SN host galaxies.

SNOC generates simulated lightcurve data with a user specified time sampling, date of discovery and noise contamination. For type Ia SNe, K-corrections for $BVRIJ$ may be calculated starting from up to 19 days prior to maximum up to 70 days past maximum in the restframe system using a spectral template from Nugent et al. (2002)[3]. For other types of SNe, approximate K-corrections are calculated from a set of (truncated) black-body functions, following the approach in Dahlén & Fransson (1999).

4.5. Simulation of supernova search conditions

Two samplings of the SN lightcurve are generated randomly using a user specified time gap. SNOC can thus be used to optimize the search strategy for finding SNe at any given redshift. The tuning parameters are the broad band filter chosen, the limiting magnitude of the search and the time between the reference and the discovery images. The method can also be used to study the contamination from core collapse SNe in the discovery sample (Dahlén & Goobar 2002).

5. The elements of the ray-tracing section

5.1. Gravitational lensing

When simulating observations of distant sources, it is necessary to take into account the fact that the Universe is inhomogeneous. First, the inhomogeneities might influence the overall expansion rate of the Universe, the so called *averaging problem*. Second, gravitational lensing effects due to the inhomogeneities will cause a dispersion in the observed source luminosities.

In SNOC we employ a method proposed by Holz & Wald (1998) for examining lensing effects. In this method, the overall expansion is assumed to follow that of the average background geometry. That is, in the following we will neglect the averaging problem and only consider effects from gravitational lensing[4].

---

[3] The spectral template of day 70 is used for later epochs.

[4] For general references on gravitational lensing see, e.g., the textbook by Schneider et al. (1992).

5.1.1. The method

The method of Holz & Wald can be summarized as follows: first, a FL background geometry is selected, i.e., we specify the space-averaged energy density content of the Universe, Ω_M and Ω_X. Inhomogeneities are accounted for by specifying matter distributions in spherical cells which have an average energy density equal to that of the underlying FL model. Thereafter, an infinitesimal beam focused at the observer is integrated backwards using the geodesic deviation equation by being sent through a series of cells, each time with a randomly selected impact parameter with respect to the matter distribution in the cell. Finally, the resulting area, A, at the source redshift is considered.

In a homogeneous FL universe, the ray bundle will have an area corresponding to the filled beam area, A_{FL}. Since the apparent luminosity of a source is proportional to the inverse of the area of the beam, we define the magnification as

$$\mu = \frac{A_{FL}}{A}. \tag{10}$$

By using Monte-Carlo techniques to trace a large number of light rays, statistics for the apparent luminosity of an ensemble of sources is obtained.

As noted in Holz & Wald, some care is needed when interpreting results as probability distributions. This is due to the fact that individual ray bundles do not correspond to random source positions. Since the fraction of the source sphere being sampled by a beam is proportional to the area of the beam, i.e., inversely proportional to the magnification, magnified sources will be over-represented if not compensated for. This is done by designating a probability proportional to the area of the ray bundle to keep each event. Further discussions of the statistical weight given to random lines-of-sight can be found in Ehlers & Schneider (1986) and Bergström et al. (2000).

In order to validate our implementation of the method, we have performed a number of consistency tests. The interested reader is referred to Bergström et al. (2000).

5.1.2. Matter distributions

The matter distribution in the cells can be chosen to be in arbitrary fractions of point-masses, uniform spheres, singular isothermal spheres (SIS) or the Navarro-Frenk-White (NFW) density profile (Navarro et al. 1997). Matter distribution parameters such as the scale radius of the NFW halo and the cut-off radius of the SIS halo are determined from distributions reflecting real galaxy properties.

One of the advantages of the method of Holz & Wald is that any mass distribution and number density, including possible redshift dependencies, can easily be implemented and used as long as the average energy density in each cell agrees with the underlying FL model.

We derive a galaxy mass distribution, dn/dM, by combining the Schechter luminosity function (see, e.g., Peebles 1993, Eq. (5.129)) with a mass-to-luminosity ratio

$$M \propto L^{\frac{1}{1-\beta}}. \tag{11}$$

For elliptical galaxies in the fundamental plane, we can, e.g., choose $\beta = 0.25$ (see Peebles 1993, Eq. (3.39)). The normalization of the resulting galaxy mass distribution, i.e., the characteristic galaxy mass, M_*, is determined from observational constraints on the galaxy number density.

5.1.3. Foreground cluster

Since all cells have the same average density as the underlying FL model, the average luminosity will be equal to the one obtained in the homogeneous case. To simulate the increased gravitational lensing effects due to a specific matter distribution along a given line-of-sight, the user can specify the properties of a cell at a given redshift to mimic a foreground galaxy or cluster. The matter distribution is in the form of an isothermal sphere,

$$\rho_{SIS}(r) = \frac{v^2}{2\pi} \frac{1}{r^2}, \tag{12}$$

where v is the line-of-sight velocity dispersion of the mass particles. Thus, the velocity dispersion sets the concentration of the cluster, the mass sets the cut-off radius and the radius of the cell sets the size of the image field.

5.1.4. Multiple images

Since we in principle only are able to follow infinitesimal light-rays in SNOC, we have to use some approximations when trying to get information on multiple image systems. The main approximation is that we assume that in cases of strong lensing, the effects from one close encounter is dominant, i.e., the one-lens approximation. With this simplification, we can use the information from the magnification to derive quantities for systems with finite separations. In order to do this, we need to be able to derive analytical relations between different observables, e.g., the magnification and the image separation. Here we show how this is done for the case of SIS lenses.

When running SNOC, we want to answer the following questions:

- Will the particular event correspond to the primary image in a multiple lens-system? If this is the case:
- What is the flux of the second image?
- What is the separation between images?
- What is the time-delay between images?

Employing the one-lens approximation with a SIS lens, we will have multiple imaging whenever $\mu_1 > 2$ and we can relate the magnification of the secondary image, μ_2, to that of the first by

$$|\mu_2| = \mu_1 - 2. \tag{13}$$

Furthermore, the image separation is given by

$$\Delta\theta = 8\pi \left(\frac{v}{c}\right)^2 \frac{D_{ds}}{D_s}, \tag{14}$$

where D_s and D_d are the angular size distances, to the source (z_s), the lens (z_d), while D_{ds} represents the angular size

distance between the lens and the source. The time delay for the two images is

$$\Delta t = \left[4\pi \left(\frac{v}{c}\right)^2\right]^2 \frac{D_{\mathrm{d}} D_{\mathrm{ds}}}{D_{\mathrm{s}}} (1 + z_{\mathrm{d}}) \frac{2}{\mu_1 - 1}. \tag{15}$$

Therefore, in order to compute the quantities of interest, we need to pick a lens redshift and velocity dispersion from some reasonable distributions for every case where $\mu_1 > 2$. The distributions will in general be functions of the cosmology, the mass distribution of the lenses and the source redshift. The differential probability for multiple imaging is in the general case given by

$$dP \propto \sigma(z_{\mathrm{d}}, z_{\mathrm{s}}) \frac{dn}{dM} dM (1 + z_{\mathrm{d}})^3 dV, \tag{16}$$

where $\sigma(z_{\mathrm{d}}, z_{\mathrm{s}})$ is the cross-section for multiple imaging and n is the comoving number density of lenses, assumed to be constant. For SIS lenses, the cross-section is given by

$$\sigma(z_{\mathrm{d}}, z_{\mathrm{s}}) \propto \left(\frac{v}{c}\right)^4 D_{\mathrm{ds}}^2. \tag{17}$$

Since $dV \propto D_{\mathrm{d}}^2 \frac{dt}{dz_{\mathrm{d}}} dz_{\mathrm{d}}$ and n is independent of lens redshift we can use

$$dP(z_{\mathrm{d}}) \propto D_{\mathrm{ds}}^2 D_{\mathrm{d}}^2 (1 + z_{\mathrm{d}})^3 \frac{dt}{dz_{\mathrm{d}}} dz_{\mathrm{d}}, \tag{18}$$

as our probability distribution for z_{d}. The probability distribution for v is given by

$$dP(v) \propto \frac{dn}{dM} \frac{dM}{dv} \left(\frac{v}{c}\right)^4 dv, \tag{19}$$

where the velocity dispersion is related to mass by

$$\frac{v}{v_*} = M^{\gamma(1-\beta)}, \tag{20}$$

(see Bergström et al. 2000, Sect. 7.1).

5.2. Extinction by dust along the line-of-sight

An important effect to consider when observing SNe is the absorption of light due to dust. With SNOC, it is possible to take the effects from three different extragalactic dust components into account:

1. A homogeneous intergalactic component;
2. A host galaxy dust component;
3. Dust in galaxies between the source and the observer.

Properties such as the exponential extinction scale-length and the frequency dependence can be set separately for each component. The frequency dependence is computed using the parametrization in Cardelli et al. (1989).

5.2.1. Grey dust

For a given emission redshift z_{s}, the attenuation Δm_{d} at observed wavelength λ_{o} due to dust can be written

$$\Delta m_{\mathrm{d}}(z_{\mathrm{s}}, \lambda_{\mathrm{o}}) = -2.5 \log_{10}\left[e^{-C \int_0^{z_{\mathrm{s}}} \rho_{\mathrm{dust}}(z) a(\lambda_{\mathrm{o}}/(1+z), R_V) h(z) dz}\right], \tag{21}$$

where $\rho_{\mathrm{dust}}(z)$ is the physical dust density at redshift z, $a(\lambda, R_V)$ is the wavelength-dependent attenuation, and the cosmology-dependent function $h(z)$ is given by

$$h(z) = [H(z)(1 + z)]^{-1}. \tag{22}$$

The reddening parameter R_V is defined by

$$A_V = R_V E(B - V), \tag{23}$$

where A_V is the V-band extinction and

$$E(B - V) = (B - V) - (B - V)_i \tag{24}$$

with $(B - V)_i$ being the intrinsic (unobscured) color.

The normalization constant C is related to the overall magnitude of the extinction, i.e., the exponential extinction scale-length[5].

In a manner similar to that used in computing gravitational lensing effects, the integral in Eq. (21) is performed numerically by following individual light paths through a large number of cells containing galaxies and intergalactic dust. Through each cell the background cosmology, the wavelength of the photon and the dust density are updated, and the contributions from each cell added. Note that the model is approximately valid also for a patchy dust distribution, as long as the scale of inhomogeneities is small enough, i.e., $1/\sqrt{N} \ll 1$ where N is the number of dust clouds intersected by the light-ray.

The intergalactic dust density is parametrized by $\rho_{\mathrm{dust}} = \rho_{\mathrm{dust}}^\circ (1 + z)^{f(z)}$, where

$$f(z) = \begin{cases} \alpha = \mathrm{const.\ for}\ z < z_{\mathrm{lim}} \\ \beta = \mathrm{const.\ for}\ z > z_{\mathrm{lim}} \end{cases} \tag{25}$$

z_{lim} is a user defined redshift where the intergalactic dust distribution is assumed to have changed properties. It is also possible to supply a user specified set of values of the dust density $\rho_{\mathrm{dust}}(z)$ and the frequency dependence as a function of redshift.

5.2.2. Host galaxy dust

The absorption in the host galaxy will be different for different SN types. This is because core collapse SNe (type II and Ibc) occur in late type, star forming, dusty galaxies whereas type Ia can occur in any type of host galaxy. In the current version of SNOC, we have used Fig. 6 in Matteucci & Recchi (2001) to make a first rough estimate of the probability for a type Ia SNe (up to $z < 4$) to occur in an early type galaxy as

$$p_{\mathrm{E}}(z) = p_{\mathrm{E}}(0) + q_1 \cdot z \tag{26}$$

where $p_{\mathrm{E}}(0) = 0.5$ and $q_1 = 0.125$. This simplistic approach could without doubt be improved on in the future.

Also, the amount of dust and the SN rate depend on the size of the galaxy (i.e., the star content). Using Monte-Carlo

---

[5] This can be fixed, e.g., by demanding that a given cosmology reproduces the observed luminosity distance at $z \sim 0.5$, i.e., that dust extinction can explain the dimming of the presently observed SN sample, otherwise attributed to the "concordance" cosmology $\Omega_{\mathrm{M}} = 0.3$, $\Omega_{\Lambda} = 0.7$.

methods, the galaxy type, dust content, SN position and disk inclination are determined and the absorption is calculated.

We model the dust distribution in late type galaxies as a double exponential disk

$$\rho_{dust} = \rho_{dust}^0 \, e^{-r/r_0 - |\zeta|/\zeta_0}, \qquad (27)$$

where r and ζ are cylindrical coordinates. We set $\zeta_0 = 0.1$ kpc. In order to determine r_0, we assume that the amount of dust is proportional to the amount of stars in the galaxy. If stars are distributed as

$$n_* = n_*^0 \, e^{-r/r_0 - |\zeta|/\zeta_0}, \qquad (28)$$

the luminosity, L, will be proportional to $\int n_* dV \propto r_0^2 \cdot \zeta_0$. If ζ_0 is fixed, we have $r_0 \propto \sqrt{L}$. That is, we set $r_0 = \sqrt{L} \, r_*^0$ where $r_*^0 = 5$ kpc is the scale radius for a $L = L_*$ galaxy. We determine ρ_{dust}^0 by setting the exponential scale-length at the galaxy center. The disk is truncated at $r_{max} = 20$ kpc and $\zeta_{max} = 3$ kpc.

We let the probability for a SN to occur in a specific galaxy be proportional to the galaxy luminosity in order to allow for SNe to be more common in star-rich, luminous galaxies. Core collapse only occur in the disk, closely following the dust distribution in Eq. (27), but we do not allow any SNe inside $r = 0.3$ kpc. We let a fraction (87.5%) of type Ia SNe follow the dust distribution in Eq. (27), only that we set $\zeta_0 = 0.35$ kpc, and the remaining fraction (12.5%) occur in a bulge according to the probability distribution

$$p(R) \propto \frac{1}{R^3 + 0.7^3}, \qquad (29)$$

where R is the radial coordinate in spherical coordinates (expressed in kpc). The bulge is truncated at $R_{max} = 3$ kpc. For further reference regarding dust and SNe distribution in host galaxies, see Hatano et al. (1998). After determining the dust distribution and SN position in the galaxy, we assume a random inclination of the disk and integrate the absorption along the path of the light-ray through the disk.

5.2.3. Dust in intervening galaxies

In each cell, the galaxy type is selected using a Monte-Carlo method. We use a parametrization where the fraction of early type, dust-free galaxies is given by $f_E(z) = f_E(0) - q_2 * z$, where $f_E(0) = 0.3$ and $q_2 = 0.05$. If the galaxy is a spiral, the absorption due to the dusty disk is computed (if the light-ray passes it). Equivalent to the case of host galaxies, we model the dust distribution in intervening spiral galaxies by a double exponential disk with random inclination, see Eq. (27).

5.3. Photon-axion oscillations

The general structure of SNOC, i.e., the tracing of light through successive cells, makes it relatively easy to add more refinement to the propagation code. As an example we mention here an exotic, hypothetical process that could affect light propagation on cosmological scales.

It has recently been proposed that the observed faintness of high-redshift SNe could be attributed to the mixing of

photons with a light axion in an intergalactic magnetic field (Csaki et al. 2001). We compute the mixing probability using the formalism of density matrices (see, e.g., Sakurai 1995). We define the mixing matrix as

$$Q = \begin{pmatrix} \Delta_\perp & 0 & \Delta_M \cos\alpha \\ 0 & \Delta_\parallel & \Delta_M \sin\alpha \\ \Delta_M \cos\alpha & \Delta_M \sin\alpha & \Delta_m \end{pmatrix}. \qquad (30)$$

The different quantities appearing in this matrix are given by

$$\Delta_\perp = -3.6 \times 10^{-25} \left(\frac{\omega}{1\,\text{eV}}\right)^{-1} \left(\frac{n_e}{10^{-8}\,\text{cm}^{-3}}\right) \text{cm}^{-1}, \qquad (31)$$

$$\Delta_\parallel = \Delta_\perp, \qquad (32)$$

$$\Delta_M = 2 \times 10^{-26} \left(\frac{B_{0,\perp}}{10^{-9}\,\text{G}}\right)\left(\frac{M_a}{10^{11}\,\text{GeV}}\right)^{-1} \text{cm}^{-1}, \qquad (33)$$

$$\Delta_m = -2.5 \times 10^{-28} \left(\frac{m_a}{10^{-16}\,\text{eV}}\right)^2 \left(\frac{\omega}{1\,\text{eV}}\right)^{-1} \text{cm}^{-1}, \qquad (34)$$

where $B_{0,\perp}$ is the strength of the magnetic field perpendicular to the direction of the photon, M_a is the inverse coupling between the photon and the axion, n_e is the electron density, m_a is the axion mass and ω is the energy of the photon. The angle α is the angle between the (projected) magnetic field and the (arbitrary, but fixed) perpendicular polarization vector. The time-evolution of the density matrix ρ is given by

$$i\delta_t\rho = \frac{1}{2\omega}[Q, \rho], \qquad (35)$$

with initial conditions

$$\rho_0 = \begin{pmatrix} \frac{1}{2} & 0 & 0 \\ 0 & \frac{1}{2} & 0 \\ 0 & 0 & 0 \end{pmatrix}. \qquad (36)$$

Here the three diagonal elements refer to two different polarization intensities and the axion intensity respectively. In each cell, we solve the 9 coupled (complex) differential equations and update ρ and Q. This method ensures that the full frequency dependence of the effect is taken into account, as shown in Mörtsell et al. (2002).

6. Fitting cosmological parameters

The SNOC package also includes a software tool for cosmology fitting, based on the output files from the Monte-Carlo program. In its current state two different types of maximum-likelihood analysis can be done using different measurement variables.

Type Ia supernovae as standard candles

The analysis tool can be used to fit the cosmological parameters $\mathcal{M}, \Omega_M, \Omega_X, \alpha_X$, and parameters related to the quintessence models presented in Goliath et al. (2001) and Eriksson & Amanullah (2002), by using simulated type Ia events where the magnitude m_i (in the redshifted B-band) and the redshift z_i are considered to be the measurement variables for each event

i. The negative log-likelihood function will in this case take the following appearance

$$\mathcal{L} = -N \ln\left(\frac{1}{\sqrt{2\pi}\sigma}\right)$$

$$+ \frac{1}{2\sigma^2} \sum_{i=1}^{N} [m_i - 5\log_{10} d'_{\mathrm{L}}(\Omega_{\mathrm{M}}, \Omega_X, \alpha; z_i) - \mathcal{M}]^2, \qquad (37)$$

where N is the number of events, σ the statistical uncertainty for each event, m_i and z_i and finally the luminosity distance, d'_{L}, is given by Eq. (4).

It is also possible to use a different, more general, likelihood function that also takes into account the fact that the data could be subject to systematic effects from gravitational lensing. This procedure is further described in Amanullah et al. (2002).

Cosmological parameters from lensed supernovae

The other way to use the analysis tool is to use lensed SNe as is described in detail in Goobar et al. (2002b). In this case core-collapse SNe as well as type Ia's can be used, and in its present state the software allows fitting of the parameters H_0, Ω_{M}, Ω_X and $\alpha_X(=\text{constant})$, by using multiply imaged high-z SNe in spherically symmetric lensing systems producing only two or ring-like images. The observables are assumed to be the source redshift, the redshift of the lensing galaxy, the image separation, $\Delta\theta$, the time delay, Δt, and the flux-ratio, r_{f}, between the images.

The negative log-likelihood function for this analysis can be expressed as

$$\mathcal{L} = \sum_{i=1}^{N} \frac{(R_{\exp}^i - \mathcal{R}^i)^2}{2\sigma^2}, \qquad (38)$$

where $R_{\exp}^i$ and $\mathcal{R}^i$ can be written as

$$R_{\exp}^i = 2\frac{\Delta t}{\Delta\theta^2}\left(\frac{1+z_{\mathrm{d}}}{f(r_{\mathrm{f}})}\right)^{-1} \quad \text{and} \qquad (39)$$

$$\mathcal{R}^i = \frac{D_{\mathrm{d}}D_{\mathrm{s}}}{D_{\mathrm{ds}}}. \qquad (40)$$

The function f depends on the flux-ratio and the applied lens model.

6.1. Minimizing the negative log-likelihood function

The user may choose between the three implemented methods to minimize the negative log-likelihood function, independently of what it looks like.

1. A simple method to minimize the negative log-likelihood function is to calculate its value in a grid, specified by start and end values for each parameter and the number of grid steps in each dimension. In the output file (see Appendix B) the result array is saved as an ASCII vector;
2. The basic idea of the *Davidon Variance Algorithm* (Davidon 1968) is to calculate the covariance matrix by an

iterative algorithm. The matrix is obtained by using only the function values and the gradient, and the minimum value is calculated simultaneously as the algorithm converges. This method is much faster in finding the minimum than the grid search, the disadvantage however, is that a parabolic shape is assumed for the negative log-likelihood function and the estimated values for the covariance matrix are somewhat misleading if this is not the case;
3. *Powell's Quadratically Convergent Method* (Powell 1964) is a multidimensional minimization algorithm that does not require any derivatives. Basically it is a method to choose in an efficient way a direction in the minimization space and then use linear minimization in that direction. This method will however not calculate any covariance matrix, only the minimum point of the function.

7. Examples of use

As an example of the usage of SNOC, we show how to create a data sample of 2000 type Ia SNe with a uniform distribution $0.1 < z < 2$ and fit the parameters Ω_{M} and α_X (assuming a flat geometry) by performing a maximum likelihood analysis.

In the SNOC input file (see Appendix A), we set:

NUMSNE	2000	
GENDIS	"uni"	
MAXZ	2.0	
MINZ	0.1	
SNTYPE	"Ia"	
INTSIG	−1.0	(default intrinsic magnitude spread)
FILTER	"BZ"	(redshifted B filter)
HUBBLE	0.65	
OMEGAM	0.3	
OMEGAX	0.7	
EOSTYPE	"con"	
ALPHAX0	−1.0	(cosmological constant)
REJTYPE	3	(keep only primary images)
DOFRAC	1	(fractional distribution of lenstypes)
FRACPOI	0.2	(20% point-masses)
FRACNFW	0.8	(80% NFW halos).

All other logical options should be set to "false" or "0". We have used a "standard" cosmology with $\Omega_{\mathrm{M}} = 0.3$ and a pure cosmological constant $\Omega_\Lambda = 0.7$ and computed lensing effects with 20% point-masses and 80% NFW halos.

In Fig. 2, we show the Hubble diagram obtained by plotting the various quantities of interest from the SNOC output ASCII file (see Appendix B). In the upper panel, the luminosity distance, d_{L}, and the lookback time $t_{\mathrm{l.b.}}$ (in units of c/H_0) are given as a function of redshift by plotting dL and lookb vs. zs.

In the lower panel, the full line is the theoretical magnitude-redshift relation for a typical type Ia SNe observed at maximum luminosity in the restframe B band. This is obtained by plotting BZmag-intsig vs. zs. In the same panel the magnitude of each individual SNe is shown, including the intrinsic dispersion and gravitational lensing effects, i.e., we have plotted BZmag+linsdm vs. zs.

We can now use the SNOC analysis tools to fit, e.g., Ω_{M} and α_X, assuming $\Omega_{\mathrm{M}} + \Omega_X = 1$.
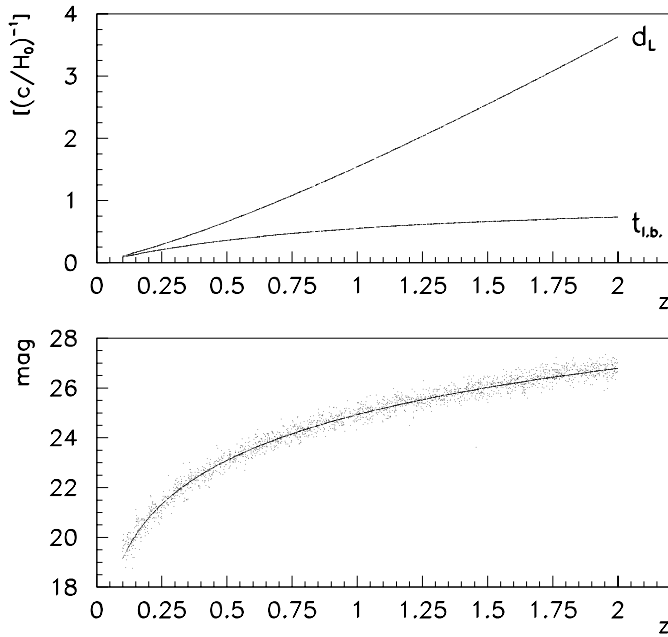
Fig. 2. In the upper panel the luminosity distance, d_L, and the lookback time $t_{\mathrm{l.b.}}$ (in units of c/H_0) are given as a function of redshift. In the lower panel the theoretical magnitude-redshift relation for type Ia SNe (full line) is plotted together with the magnitude of each individual SNe including the intrinsic dispersion and gravitational lensing effects.

In the input for the analysis tool (Appendix A), we set:

```
nrsne           2000
nrparsigma      2
flat            (assuming Ω_M + Ω_X = 1)
w_0             −1.0 0.0 200 −1
omega_M         0.0 0.4 200 0.3
NUISM
 nointsig
gauss
nodavidonmin
gridsearch
nopowellmin
```

Figure 3 shows the confidence contours produced from this three-parameter fit, where $\mathcal{M}$ has been treated as a nuisance parameter. The solid contour that is centred around the input values $\Omega_\mathrm{M} = 0.3$, and $\alpha_X = -1.0$ is the fitted confidence region when the lensing dispersion is not considered, i.e., the keyword `nolenseffect` has been specified in the input file. The dashed contour shows instead the fitted result when the `addlenseffect` parameter has been specified in the input file and the lensing effects are considered. As can be seen, this will induce a significant bias in the parameter determination, an effect discussed in further detail in Amanullah et al. (2002).
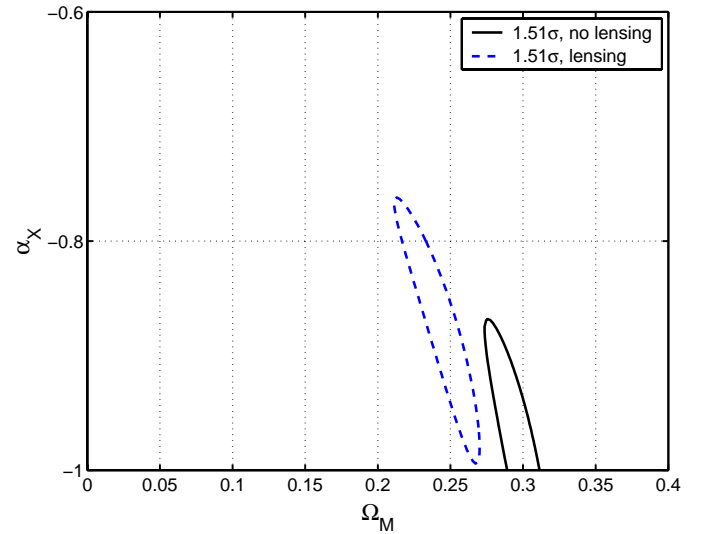
Fig. 3. Three-parameter fits in the $(\Omega_\mathrm{M}, \alpha_x)$-plane using the data set shown in Fig. 2. The contours show the 1.51σ level, which corresponds to a probability content of ~68% of including both parameter in the region.

Both contours show the

$$\min(\mathcal{L}) + \frac{1.51^2}{2}$$

level of the negative log-likelihood surface, $\mathcal{L}$, defined in Eq. (37). This level corresponds approximately to a confidence region of ~68% of including the true value of the two parameters of interest.

8. Summary

As we enter a phase of high-precision cosmological measurements, sophisticated tools for data analysis are required, especially to evaluate potential systematic effects related to the method. The Monte-Carlo simulation package SNOC is mainly designed for the study of the precision and possible biases of measured cosmological parameters from high-z type Ia SNe. Besides calculating the luminosity distance for arbitrary cosmological parameters: $H_0, \Omega_\mathrm{M}, \Omega_X, \alpha_X(z)$, the code also allows for the estimates of observed magnitudes for high-z SNe taking into account the inhomogeneity of matter and dimming by, e.g., dust or more exotic process such as photon-axion oscillations. Along with the simulation, a maximum-likelihood analysis package has been developed for fitting of cosmological parameters and possible bias.

Appendix A: Appendix A: Summary of SNOC input parameters

The input for the Monte-Carlo tool

Table A.1. The SNOC Monte-Carlo tool steering parameters.

parameter name	description
NUMSNE	number of SNe to be generated
SEED	seed for random number generator (if negative use computer clock)
SNTYPE	SN type
Redshift distribution	
GENDIS	functional form of SN redshift distribution option
MEANZ	mean redshift of SN sample (for Gaussian distribution only)
SIGMAZ	σ in redshift of SN sample (for Gaussian distribution only)
MAXZ	maximum SN redshift
MINZ	minimum SN redshift
ZFILE	name of file with tabulated z-distribution of SNe (optional)
TAUIA	τ-parameter to in SFR redshift distribution (Dahlén & Fransson 1999)
Lightcurve	
INTSIG	intrinsic magnitude spread of SNe
BUILDLC	option to build SN lightcurves
LCPOINT	number of points in lightcurve (optional)
LCNOISE	measurement error in each lightcurve point
LCSPACE	number of days between lightcurve points
LCTMIN	earliest day in lightcurve
FILTER	default filter for lightcurve (*BVRIJ*)
USFILT	user specified filters
STRETCH	lightcurve "stretch", relevant for type Ia SNe (Perlmutter et al. 1997)
STRCORR	lightcurve "stretch-brightness" correlation (Perlmutter et al. 1997)
STRSIG	intrinsic lightcurve "stretch" standard deviation
Cosmological parameters	
HUBBLE	Hubble parameter, h ($H_0 = h \cdot 100$ km s^{-1} Mpc^{-1})
OMEGAM	mass density, $\Omega_M(z = 0)$
OMEGAX	dark energy, $\Omega_X(z = 0)$
EOSTYPE	dark energy equation of state form (constant or time varying)
ALPHAX0	dark energy equation of state parameter, $w_0 = p_X/\rho_X$ at $z = 0$
ALPHAX1	dark energy equation of state parameter, first derivative, $w_1 = \frac{dw}{dz}$
EOSFILE	dark energy equation of state parameter, tabulated file with $w(z)$ (optional)
Gravitational lensing	
LENS	parametrization of matter lenses (compact objects, uniform, SIS or NFW)
DOFRAC	option to use alternating lens types
FRACHOM	fraction of path in homogeneous matter
FRACPOI	fraction of path in an environment of compact objects
FRACUNI	fraction of path in an environment of uniform objects
FRACISO	fraction of path in an environment of SIS mass distributions
FRACNFW	fraction of path in an environment of NFW mass distributions
CELLSZ	initial cell size [Mpc] (when MTYPE 1)
MATTERB	size of homogeneous matter ball [Mpc] (when LENS "uni")
MULTI	option to treat multiple images of gravitationally lensed SNe
REJTYPE	event rejection level for secondary (lensed) images
CLUSTER	option to simulate lensing due to foreground galaxy cluster
ZCL	redshift of foreground galaxy cluster
VELDISP	dispersion velocity of foreground galaxy cluster
MASSCLU	mass of foreground galaxy cluster
RADCLU	radius of foreground cluster image field
Dust extinction	
DOGREY	option to add intergalactic dust in the line-of-sight

MINWAVE	shortest observable wavelength
MAXWAVE	longest observable wavelength
NUMPOI	number of points in the wavelength range
GREYTAB	option to use tabulated grey dust parameters vs redshift
GDFILE	file with grey dust tabulated data
RV	intergalactic dust parameter, see Eq. (23)
GREYSC	mean free path for intergalactic dust scattering
ZLIM	turning redshift in dust model, see Eq. (25)
P1	exponent in dust density redshift evolution below ZLIM, see Eq. (25)
P2	exponent in dust density redshift evolution above ZLIM, see Eq. (25)
DOHOST	option to simulate host galaxy type, brightness and dust extinction
RVHOST	R_V for host galaxy dust
HOSTSC	mean free path for host galaxy dust scattering
DOGLXY	option to consider dust extinction from foreground galaxies
RVGLXY	R_V for foreground galaxy dust
GLXYSC	mean free path for foreground galaxy dust scattering
Photon-axion oscillations	
DOMIX	option to consider photon-axion oscillations
B0	mean comoving magnetic field
B0WID	width of uniform dispersion of magnetic field
MMA	strength of photon-axion coupling
MA	axion mass
NE	mean comoving electron density
NEWID	width of uniform dispersion of electron density
K-corrections	
DOKCORR	calculate K-corrections at maximum from restframe B to observed $BVRIJ$
KFULL	write out magnitude distortions from host galaxy dust or line-of-sight dust
Galaxy parameters	
EVOLUM	evolution if host galaxy luminosities according to $L(z) = L(0)(1 + z)^{\text{EVOLUM}}$
MTYPE	equal mass galaxies or weighted by Schechter function
SCHEAL	Schechter function parameter
SN search	
DOSEAR	option to simulate search conditions
TIMEGAP	time between reference and discovery images in search mode

The input for the analysis tool

Table A.2. SNOC analysis steering parameters.

parameter name	description
nrsne	number of SNe to use in the fit
zrange	only use SNe within specified z-range
nrparsigma	the number of parameters that should simultaneously lie within a specific deviation range
flat	assume that the Universe is flat
noflat	do not assume that the Universe is flat
Fit parameters	

These parameters specify which of the cosmological parameters that should be fixed and which that should be fitted. Each line consist of a parameter name and four numerical values, s, e, g and c. For a parameter to be fitted s and e cannot be identical, and g should be an integer greater than 1. For a grid search s and e specifies the grid interval for each parameter and g then number of steps. The value c should be the correct value of each parameter that was used in the Monte-Carlo. For the iterative minimization methods a start value will randomly be selected between s and e.

w_0 s e g c	non-redshift dependent part of the equation of state parameter

`w_1 s e g c`	linearly redshift dependent part of the equation of state parameter
`omega_M s e g c`	mass density, Ω_M ($z = 0$)
`omega_X s e g c`	dark energy, Ω_X ($z = 0$)
`mscript s e g c`	intercept in the Hubble diagram, $\mathcal{M}$, only used for Hubble diagram fits
`hubble0 s e g c`	Hubble parameter, h ($H_0 = h \cdot 100$ km s^{-1} Mpc^{-1}), only used for fits of multiply imaged objects

Nuisance parameters	
`NUISM`	fit $\mathcal{M}$ as a nuisance parameter
`NUIFP`	fit the fraction of compact objects in the Universe

type Ia fits	
`gausserror`	the uncertainty in the magnitude σ
`addintsig`	add a dispersion to the measured magnitudes
`nointsig`	do not add a dispersion to the measured magnitudes
`addlenseffect`	add the magnitude dispersion due to lensing
`nolenseffect`	do not add the magnitude dispersion due to lensing
`magresiduals`	calculate the magnitude residuals from the best cosmology fit
`nomagresiduals`	do not calculate the magnitude residuals from the best cosmology fit
`gauss`	assume Gaussian magnitude distribution
`gausslin`	assume a modified Gaussian magnitude distribution to handle gravitational lensing

Multiple image fits	
`domulti`	do a multiple image fit instead of the default type Ia fit
`ibandmax`	maximum allowed I-band magnitude for the SNe
`lenstype`	which lens model to use, SIS or POI
`etimedelay`	uncertainty in the time delay in days
`eimsep`	uncertainty in the image separation in arcsecs
`imrat`	uncertainty in the flux ratio
`ezl`	uncertainty on lensing galaxy redshift
`emodel`	systematic error on lensing model

Minimization method	
`davidonmin`	use the Davidon Variance Algorithm
`nodavidonmin`	do not use the Davidon Variance Algorithm
`gridsearch`	use the grid search
`nogridsearch`	do not use the grid search
`powellmin`	use Powell's Quadratically Convergent Method
`nopowellmin`	do not use Powell's Quadratically Convergent Method

Appendix B: Appendix B:The SNOC output

The output of the Monte-Carlo tool

SNOC produces an ASCII output file that can be easily interpreted and piped into histogramming tools[6]. Table B.1 shows the first event record of a SNOC simulation.

Table B.1. Extract of SNOC output showing the first event record.

SNOC output file: example

variable	value	description
`event`	1	event number
`sntype`	"Ia"	SN type
`hubble`	0.6500	Hubble parameter
`omegam`	0.2800	$\Omega_M(z = 0)$
`omegax`	0.7200	$\Omega_X(z = 0)$
`alphax0`	−1.0000	$w_0(z = 0)$
`Ntotal`	237	number of SNe sq deg^{-1} year^{-1}

---

[6] We use the CERNLIB package PAW for that purpose.

nzbins	28	number of *z*-bins for rates
zcent	0.125 0.175 0.225 0.275 0.325 0.375	center of *z*-bin
	0.425 0.475 0.525 0.575 0.625 0.675	
	0.725 0.775 0.825 0.875 0.925 0.975	
	1.025 1.075 1.125 1.175 1.225 1.275	
	1.325 1.375 1.425 1.475	
zrate	0.749 1.414 2.154 2.770 3.741 4.576	differential SN rate
	5.076 6.144 6.896 7.161 8.218 8.818	
	8.828 9.824 10.260 10.043 10.961 11.250	
	10.850 11.688 11.856 11.319 12.083	
	12.156 11.523 12.223 12.223 11.527	
zs	0.4318	redshift of SN (in event #1)
lookb	0.3264	lookback time (Hubble time units)
lookGyr	4.9234	lookback time in Giga-years
dL	0.5586	luminosity distance in units of $\frac{c}{H_0}$
BZmag	22.9903	effective *B*-band magnitude of event
intsig	0.2662	intrinsic *B*-band offset from mean *B*-band Ia magnitude
emptyb	1.0241	luminosity ratio empty beam/filled beam
emptydm	0.0259	magnitude offset empty beam – filled beam
lensrat	1.0212	lensing flux ratio demagnification
linsdm	0.0228	lensing demagnification (magnitude)
ncells	386	number of galaxy cells along path
ncaustics	0	number of parity-inversions of image along path
nreject	0	number of image rejections before keeping event
ttot	1508.5641	travel time (Mpc)
galtype	'Sbc'	host galaxy type
galabsB	−16.4987	host galaxy absolute magnitude
galBband	26.2917	host galaxy *B*-band magnitude
galVband	25.0382	host galaxy *V*-band magnitude
galRband	24.2002	host galaxy *R*-band magnitude
galIband	23.5455	host galaxy *I*-band magnitude
hostdm	0.0000	effective *B*-band extinction in host
greysc	58200.000	intergalactic dust mean free path (Mpc)
r_v	9.5000	R_V intergalactic dust
zgreylim	0.5000	intergalactic dust, density turn-point, see Eq. (25)
greyexp1	3.0000	intergalactic dust, exponent below turn-point, see Eq. (25)
greyexp2	0.0000	intergalactic dust, exponent above turn-point, see Eq. (25)
greydm	0.5118	intergalactic dust magnitude extinction of effective *B*-band
numgrey	30	number of wavelength bins for intergalactic reddening
lambdagr	4000.0 4448.3 4896.6 5344.8 5793.1	wavelength central value
	6241.4 6689.7 7137.9 7586.2 8034.5	
	8482.8 8931.0 9379.3 9827.6 10275.9	
	10724.1 11172.4 11620.7 12069.0	
	12517.2 12965.5 13413.8 13862.1	
	14310.3 14758.6 15206.9 15655.2	
	16103.4 16551.7 17000.0	
greyvec	0.539E-01 0.558E-01 0.560E-01 0.548E-01 0.532E-01 0.514E-01 0.496E-01	differential extinction
	0.476E-01 0.456E-01 0.436E-01 0.415E-01 0.395E-01 0.375E-01 0.356E-01	
	0.337E-01 0.318E-01 0.300E-01 0.283E-01 0.267E-01 0.252E-01 0.239E-01	
	0.226E-01 0.214E-01 0.204E-01 0.194E-01 0.185E-01 0.176E-01 0.168E-01	
	0.161E-01 0.154E-01	

mixdm	0.2443	effective B-band extinction due to photon-axion oscillations
KcorBB0	1.2692	K_{BB}-correction, LC maximum
KcorBV0	−0.1974	K_{BV}-correction, LC maximum
KcorBR0	−0.7003	K_{BR}-correction, LC maximum
KcorBI0	−0.7416	K_{BI}-correction, LC maximum
KcorBJ0	−0.1928	K_{BJ}-correction, LC maximum
KcorBB1	1.2808	K_{BB}-correction (includes host galaxy extinction)
KcorBV1	−0.1873	K_{BV}-correction (includes host galaxy extinction)
KcorBR1	−0.6916	K_{BR}-correction (includes host galaxy extinction)
KcorBI1	−0.7349	K_{BI}-correction (includes host galaxy extinction)
KcorBJ1	−0.1892	K_{BJ}-correction (includes host galaxy extinction)
KcorBB2	1.2692	K_{BB}-correction (includes foreground galaxy extinction)
KcorBV2	−0.1974	K_{BV}-correction (includes foreground galaxy extinction)
KcorBR2	−0.7003	K_{BR}-correction (includes foreground galaxy extinction)
KcorBI2	−0.7416	K_{BI}-correction (includes foreground galaxy extinction)
KcorBJ2	−0.1928	K_{BJ}-correction (includes foreground galaxy extinction)
KcorBB3	1.3246	K_{BB}-correction (includes intergalactic extinction)
KcorBV3	−0.1434	K_{BV}-correction (includes intergalactic extinction)
KcorBR3	−0.6500	K_{BR}-correction (includes intergalactic extinction)
KcorBI3	−0.6978	K_{BI}-correction (includes intergalactic extinction)
KcorBJ3	−0.1665	K_{BJ}-correction (includes intergalactic extinction)
KcorBB4	1.4405	K_{BB}-correction (includes photon-axion oscillation)
KcorBV4	−0.0273	K_{BV}-correction (includes photon-axion oscillation)
KcorBR4	−0.4390	K_{BR}-correction (includes photon-axion oscillation)
KcorBI4	−0.4464	K_{BI}-correction (includes photon-axion oscillation)
KcorBJ4	0.1988	K_{BJ}-correction (includes photon-axion oscillation)
KcorBB	1.5257	K_{BB}-correction total extinction folded
KcorBV	0.0546	K_{BV}-correction total extinction folded
KcorBR	−0.3646	K_{BR}-correction total extinction folded
KcorBI	−0.3843	K_{BI}-correction total extinction folded
KcorBJ	0.2350	K_{BJ}-correction total extinction folded
stretch	0.9457	lightcurve stretch
strcorr	0.0543	stretch-brightness correction
npoints	8	number of lightcurve points
lcdate	−13.54 −6.77 0.00 6.77 13.54 20.31 27.08 33.85	dates from maximum
lcmag	0.42 −0.05 −0.58 −0.28 0.13 0.54 1.15 1.61	$m_R(t)$ − BZmag (R-band lightcurve)
lcnoise	0.1000	applied noise standard deviation in LC points
dayref	−12.1837	days from maximum for reference image (rest frame)
daynew	3.1770	days from maximum for search image (rest frame)
magdiffB	−0.9194	SN B-band magnitude difference new – ref epoch
magdiffV	−1.2900	SN V-band magnitude difference new – ref epoch
magdiffR	−1.4338	SN R-band magnitude difference new – ref epoch
magdiffI	−1.5398	SN I-band magnitude difference new – ref epoch
magdiffJ	−1.3374	SN J-band magnitude difference new – ref epoch
magnewB	1.5924	SN B-band magnitude (-BZmag) at discovery epoch
magnewV	−0.0228	SN V-band magnitude (-BZmag) at discovery epoch
magnewR	−0.6042	SN R-band magnitude (-BZmag) at discovery epoch
magnewI	−0.7418	SN I-band magnitude (-BZmag) at discovery epoch
magnewJ	−0.0819	SN J-band magnitude (-BZmag) at discovery epoch
end		end of event # 1

The output of the analysis tool

SNOC output file: example

```
# THIS IS THE OUTPUT GENERATED BY SNALYS
# ======================================
# The number of supernovae used:    2300
# The number of parameters estimated:  2

# Flat universe assumption: no
# Execution started at: Wed Mar  6 16:24:15 2002
# Total execution time: 00:01:33.00
# Used CPU-time: total = 00:01:35.43
#                user = 00:01:35.34
#                system = 00:00:00.07


# Powell Minimization
# ===================
# Start values
omega_m      0.333
omega_x      0.733
# The min of the ML function (powell):      0.010
# Cosmology (powell)
omega_m      0.299860
omega_x      0.699683


# Davidon Minimization
# ====================
# Start values
omega_m      0.300
omega_x      0.700
# The min of the ML function (davidon):      0.010
# Cosmology (davidon)
omega_m    0.299983 +/-  0.023836
omega_x    0.699974 +/-  0.046131
# Correlation matrix (davidon)
          omega_m    omega_x
omega_m     1.00000    0.95052
omega_x     0.95052    1.00000


# Grid Search
# ===========
# The min of the ML function (grid):      6.729
# Cosmology (grid)
omega_m    0.333333 +   0.33E-01 -   0.67E-01
omega_x    0.733333 +   0.00E+00 -   0.67E-01
# Conditions for grid search.
# Parameter        start    stopnr.step
    omega_m    0.10 0.40    10
    omega_x    0.40 1.00    10
# The ML-function from Grid Search
#omega_m   omega_x
  82.4738235
  42.1675644
  51.1707954
  ...
```

References

Amanullah, R., Mörtsell, E., & Goobar, A. 2002, A&A, submitted [astro-ph/0204280]

Bergström, L., & Goobar, A. 1999, Cosmol. Part. Astrophys. (Wiley/Praxis, Chichester)

Bergström, L., Goliath, M., Goobar, A., & Mörtsell, E. 2000, A&A, 358, 13

Cardelli, J. A., Clayton, G. C., & Mathis, J. S. 1989, ApJ, 345, 245

Coleman, G. D., Wu, C. C., & Weedman, D. W. 1980, ApJS, 43, 393

Csaki, C., Kaloper, N., & Terning, J. 2002, Phys. Rev. Lett., 88, 161 302

Dahlén, T., & Fransson, C. 1999, A&A, 350, 349

Dahlén, T., & Goobar, A. 2002, PASP, 114, 284

Davidon, W. C. 1968, Comp. J., 10, 406

Ehlers, J., & Schneider, P. 1986, A&A, 168, 57

Eriksson, M., & Amanullah, R. 2002, Phys. Rev. D, in press [astro-ph/0202157]

Goliath, M., Amanullah, R., Astier, P., Goobar, A., & Pain, R. 2001, A&A, 380, 6

Goliath, M., & Mörtsell, E. 2000, Phys. Lett. B, 486, 249

Goobar, A., & Perlmutter, S. 1995, ApJ, 450, 14

Goobar, A., Bergström, L., & Mörtsell, E. 2002a, A&A, 384, 1

Goobar, A., Mörtsell, E., Amanullah, R., & Nugent, P. 2002b, A&A, in press

Hatano, K., Branch, D., & Deaton, J. 1998, ApJ, 502, 177

Holz, D. E., & Wald, R. M. 1998, Phys. Rev. D, 58, 063 501

Kim, A., Goobar, A., & Perlmutter, S. 1996, PASP, 108, 190

Matteucci, F., & Recchi, S. 2001, ApJ, 558, 351

Mörtsell, E., Goobar, A., & Bergström, L. 2001a, ApJ, 559, 53

Mörtsell, E., Gunnarsson, C., & Goobar, A. 2001b, ApJ, 561, 106

Mörtsell, E., Bergström, L., & Goobar, A. 2002, Phys. Rev. D, in press [astro-ph/0202153]

Navarro, J. F., Frenk, C. S., & White, S. D. M. 1997, ApJ, 490, 493

Nugent, P., Kim, A., & Perlmutter, S. 2002, PASP, in press [astro-ph/0205351]

Peebles, P. J. E. 1993, Principles of physical cosmology (Princeton University Press, Princeton)

Perlmutter, S., Gabi, S., Goldhaber, G., et al. 1997, ApJ, 483, 565

Perlmutter, S., Aldering, G., Goldhaber, et al. 1999, ApJ, 517, 565

Powell, M. J. D. 1964, Comp. J., 7, 155

Riess, A. G., Filippenko, A. V., Challis, P., et al. 1998, AJ, 116, 1009

Riess, A. G., Nugent, P., Gilliland, R. L., et al. 2001, ApJ, 560, 49

Sakurai, J. J. 1995, Modern Quantum Mechanics, Reading

Schneider, P., Ehlers, J., & Falco, E. E. 1992, Gravitational Lenses (Springer-Verlag, Berlin)

Walck, Ch., http://www.physto.se/˜walck/suf.html